JCTC Journal of Chemical Theory and Computation

Article

pubs.acs.org/JCTC

DFTB Parameters for the Periodic Table, Part 2: Energies and Energy Gradients from Hydrogen to Calcium

Augusto F. Oliveira,[†] Pier Philipsen,[‡] and Thomas Heine*[,†,§]

[†]Department of Physics & Earth Sciences, Jacobs University Bremen, Campus Ring 1, 28759 Bremen, Germany

[‡]Scientific Computing & Modelling NV, Theoretical Chemistry, Vrije Universiteit, De Boelelaan 1083, 1081 HV Amsterdam, The Netherlands

[§]Wilhelm-Ostwald-Institut für Physikalische und Theoretische Chemie, Universität Leipzig, Linnéstr. 2, 04103 Leipzig, Germany

Supporting Information

ABSTRACT: In the first part of this series, we presented a parametrization strategy to obtain high-quality electronic band structures on the basis of density-functional-based tight-binding (DFTB) calculations and published a parameter set called QUASINANO2013.1. Here, we extend our parametrization effort to include the remaining terms that are needed to compute the total energy and its gradient, commonly referred to as repulsive potential. Instead of parametrizing these terms as a two-body potential, we calculate them explicitly from the DFTB analogues of the Kohn−Sham total energy expression. This strategy requires only two further numerical parameters per element. Thus, the atomic configuration and four real numbers per element are sufficient to define the DFTB model at this level of parametrization. The QUASINANO2015 parameter set allows the calculation of energy, structure, and electronic structure of all systems composed of elements ranging from H to Ca. Extensive benchmarks show that the overall accuracy of QUASINANO2015 is comparable to that of well-established methods, including PM7 and hand-tuned DFTB parameter sets, while coverage of a much larger range of chemical systems is available.

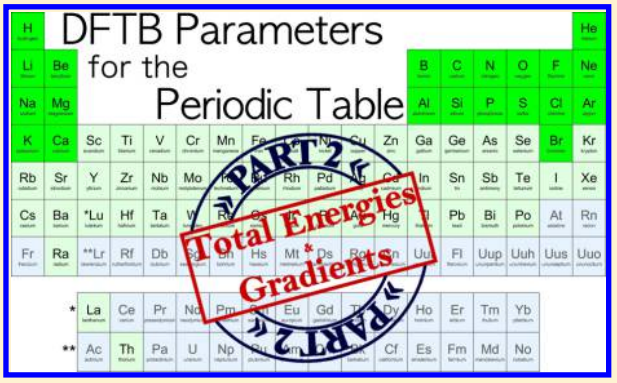

1. INTRODUCTION

Density-functional-based tight-binding (DFTB), first introduced by Seifert, Eschrig, and Bieger in the 1980s,[1] is an approximate method based on the Kohn−Sham (KS) approach to density functional theory.[2,3] Along the years, the method has been extended and improved in various ways, thus becoming applicable to a wide range of materials, including systems with heterogeneous covalent bonds,[4] van der Waals interactions,[5−9] spin polarization and spin−orbit coupling,[10,11] etc. The recent development of DFTB3 resulted in unprecedented accuracy in structure and reaction energies of organic and bioorganic molecules.[12−14] However, all flavors of DFTB require parameters that are traditionally generated using significant manual effort. As a result, DFTB parameters are not available for the entire periodic table and, thus, the applicability of the method is restricted to selected system classes.

One of the biggest challenges regarding the DFTB parametrization is the formulation of the total energy, historically done in an effective additive two-body potential form. This requires the generation of $N(N + 1)/2$ parameter sets for a system containing N chemical elements (one parameter set for each element pair); thus, DFTB for the periodic table would require more than 5000 parameter sets. In order to avoid such extensive effort, we pursue a formulation in which the DFTB parameters are atomically defined so that the number of parameter sets becomes equal to the number of elements in the system.

In the first article of this series,[15] we have presented a semiautomatic parametrization procedure for the DFTB electronic part, yielding the KS-like wave functions. With those, all related quantities can be calculated, including electron density, orbital energies and other expectation values, and, in the case of crystals, electronic band structures. Parameters for most of the elements in the periodic table (the main exceptions being the elements with f valence orbitals) have been proposed and validated on band structures of various systems. In addition, we have shown that a list specifying the atomic electron configuration and two additional parameters for each element is sufficient to define the DFTB electronic terms for the periodic table.

For the calculation of the total energy, additional terms are required. These are dominated by repulsive contributions and, therefore, are generally referred to as repulsion energy or repulsion potential. In this article, we develop a parametrization concept that allows the repulsion energy to be calculated directly from the DFTB Kohn−Sham-like equations. Following the same idea used in the procedure developed for the

Received: July 23, 2015
Published: October 7, 2015

DOI: 10.1021/acs.jctc.5b00702
J. Chem. Theory Comput. 2015, 11, 5209−5218

electronic energy in Part 1,[15] we have avoided the common two-center parametrization in which the energy difference between DFTB and DFT benchmark calculations is minimized by introducing diatomic potential functions (see Short Review of DFTB and SCC-DFTB below). Using similar principles as those involved in the preliminary works of Mirtschink[16] and Bodrog,[17] we have developed an alternative approach where the repulsion energy contributions are completely defined from one-center parameters. We will show that two additional real numbers per element are sufficient to define the repulsion energy.

On the basis of this strategy, we present a complete set of DFTB parameters for the calculation of total energies and gradients comprising the first 20 elements of the periodic table (H to Ca). The new parameter set, named QUASINANO2015, uses the same electronic parameters presented in Part 1[15] and has been optimized for providing high-quality structures of finite and periodic systems.

The remainder of this article is organized as follows: First, we briefly review the DFTB method, giving special emphasis to the repulsion energy. Next, we present our approach to calculate the repulsion energy, followed by the detailed description of our parametrization strategy for the repulsion contributions. We then present the QUASINANO2015 parameters, developed in this work, and assess their quality and transferability by comparing them with DFTB results obtained with the MATSCI-0-3[18] and MIO-1-1[4,12,19] parameter sets and PM7[20] calculations. Finally, we present our conclusions and final remarks.

2. SHORT REVIEW OF DFTB AND SCC-DFTB

In the first part[15] of this article series, we have briefly reviewed the DFTB method, with emphasis on the KS orbitals and electronic energy. Here, we extend this short review in order to establish the grounds for developing our new parametrization strategy, with a focus on the remaining terms that define the total energy, i.e., the so-called repulsion energy. For the reader seeking more general information about DFTB and its approximations, we suggest several review papers available in the literature.[21−23]

DFTB can be interpreted as an approximation of the KS density functional method,[3] in which the total energy is expressed as a sum of two contributions

$$E = E_{\mathrm{ele}} + E_{\mathrm{rep}} \tag{1}$$

where E_{ele} and E_{rep} are the electronic and repulsion energies, respectively.

In order to obtain eq 1, the total electron density ρ is written in terms of a reference density ρ_0 subject to a density perturbation $\Delta\rho$, i.e.

$$\rho(\vec{r}) = \rho_0(\vec{r}) + \Delta\rho(\vec{r}) \tag{2}$$

In addition, the DFT exchange-correlation energy functional E_{xc} is approximated as a second-order Taylor series expansion

$$E_{\mathrm{xc}}[\rho_0 + \Delta\rho] = E_{\mathrm{xc}}[\rho_0] + \int \frac{\delta E_{\mathrm{xc}}}{\delta\rho_0}\Delta\rho \,\mathrm{d}\vec{r} + \frac{1}{2}\iint \frac{\delta^2 E_{\mathrm{xc}}}{\delta\rho_0{}'\delta\rho_0}\Delta\rho'\Delta\rho \,\mathrm{d}\vec{r}'\,\mathrm{d}\vec{r} \tag{3}$$

where $\rho = \rho(\vec{r})$ and $\rho' = \rho(\vec{r}')$. Then, using eqs 2 and 3, the KS density functional can be written as

$$E[\rho_0 + \Delta\rho] = \underbrace{\sum_i^N \langle\psi_i|\hat{H}^0|\psi_i\rangle}_{E_0} + \underbrace{\frac{1}{2}\iint\left(\frac{1}{|\vec{r}-\vec{r}|} + \frac{\delta^2 E_{\mathrm{xc}}[\rho_0]}{\delta\rho\delta\rho'}\right)\Delta\rho\Delta\rho' \,\mathrm{d}\vec{r}\,\mathrm{d}\vec{r}'}_{E_{\mathrm{scc}}} \underbrace{- \frac{1}{2}\iint\frac{\rho_0\rho_0'}{|\vec{r}-\vec{r}'|}\,\mathrm{d}\vec{r}\,\mathrm{d}\vec{r}' + E_{\mathrm{xc}}[\rho_0] - \int v_{\mathrm{xc}}\rho_0 \,\mathrm{d}\vec{r} + E_{\mathrm{nn}}}_{E_{\mathrm{rep}}} \tag{4}$$

corresponding to three energy contributions: the electronic energy term (E_0), a charge fluctuation correction to the electronic energy (E_{scc}), present in SCC-DFTB[4] and DFTB3,[12] and the repulsion energy (E_{rep}).

The KS equations are formulated within the LCAO ansatz, where the electronic eigenstates ψ_i are calculated from a linear combination of atomic valence orbitals ϕ_μ

$$\psi_i(\vec{r}) = \sum_\mu c_{\mu i}\phi_\mu(\vec{r}) \tag{5}$$

Thus, the E_0 term becomes

$$E_0 = \sum_i n_i \sum_\mu \sum_\nu c_{\mu i}c_{\nu i}H^0_{\mu\nu} = \mathrm{Tr}(\mathbf{P}\cdot\mathbf{H^0}) \tag{6}$$

which describes the E_{ele} term in eq 1, with n_i being the occupation number of the ith eigenstate and $\mathbf{P}$ being the density matrix. Details of the approximations used in the construction of the Hamiltonian matrix $\mathbf{H^0}$ (in particular, the two-center approximation) have been discussed in Part 1.[15]

Within SCC-DFTB,[4] the charge density fluctuation yields the E_{scc} term in eq 4, approximated as

$$E_{\mathrm{scc}} = \frac{1}{2}\sum_A\sum_B \gamma_{AB}(R_{AB})q_Aq_B \tag{7}$$

where q_A and q_B are atomic Mulliken charges and γ_{AB} is an analytical function interpolating two limiting cases of E_{scc}: $R_{AB} \to 0$ and $R_{AB} \to \infty$. From this approximation, a new Hamiltonian matrix $\mathbf{H}$ can be developed,[4] with elements

$$H_{\mu\nu} = H^0_{\mu\nu} + \underbrace{\frac{1}{2}S_{\mu\nu}\sum_K(\gamma_{AK} + \gamma_{BK})q_K}_{V^{\mathrm{scc}}_{\mu\nu}} \tag{8}$$

where $H^0_{\mu\nu}$ are the elements from the $\mathbf{H^0}$ matrix in eq 6 and $S_{\mu\nu} = \langle\phi_\mu|\phi_\nu\rangle$. Thus, the electronic energy term in eq 1 is redefined as

$$E_{\mathrm{ele}} = \sum_i n_i \sum_\mu \sum_\nu c_{\mu i}c_{\nu i}(H^0_{\mu\nu} + V^{\mathrm{scc}}_{\mu\nu}) = \mathrm{Tr}(\mathbf{P}\cdot\mathbf{H^0}) + \mathrm{Tr}(\mathbf{P}\cdot\mathbf{V^{scc}}) \tag{9}$$

It should be noted that the extra parameters required for the calculation of the $\mathbf{V^{scc}}$ matrix are not free; they are, rather, the atomic chemical hardnesses, the derivative of the pseudoatomic energies with respect to their electron occupation numbers,

DOI: 10.1021/acs.jctc.5b00702
J. Chem. Theory Comput. 2015, 11, 5209−5218

calculated directly from DFT using Janak's theorem.[24] Therefore, although density matrix **P** and MO coefficients might be different, the $\mathbf{H}^0$ matrix is the same for both DFTB and SCC-DFTB.

In the remainder of this article, we discuss only SCC-DFTB results, which coincide, for some high-symmetry single-element species, with DFTB. Thus, we will use the terms SCC-DFTB and DFTB synonymously.

The crucial component of the parametrization concept is the construction of the atomic orbitals and the effective potential defining the Hamiltonian operator in the KS-like DFTB equations. The common strategy is to solve the KS equations for spherical pseudoatoms subject to a confinement potential in the form

$$v_{\mathrm{conf}}^{A}(r) = \left(\frac{r}{r_0^A}\right)^{\sigma_A} \tag{10}$$

that is

$$\left[\hat{T} \underbrace{-\frac{Z_A}{r} + \int \frac{\rho_0^A(\vec{r}')}{|\vec{r} - \vec{r}'|}\mathrm{d}\vec{r} + v_{\mathrm{xc}}[\rho_0^A] + v_{\mathrm{conf}}^A(r)}_{V_{\mathrm{eff}}^A}\right]\phi_\mu^A(\vec{r}) = \varepsilon_\mu^A \phi_\mu^A(\vec{r}) \tag{11}$$

which is solved self-consistently for each element in its representation as pseudoatom A. The solution of eq 11 (the atomic orbitals ϕ_μ^A, the effective potential V_{eff}^A, and the atomic electron density ρ_0^A) defines the DFTB equations.

In Part 1,[15] we have used v_{conf}^A as the term to be optimized by varying the atomic confinement radii r_0^A and exponents σ_A until the electronic band energies and curvatures of a series of reference solids matched PBE/TZP reference calculations as closely as possible. Thus, the electronic part of the total energy in either DFTB or SCC-DFTB is already available within the QUASINANO2013.1 parameter set.[15]

The remaining contribution to the total energy, E_{rep}, corresponds to the DFT double-counting terms and the internuclear repulsion E_{nn} (eq 4). The latter is calculated exactly, within the classical limits and point-charge approximation, from the atomic numbers Z and interatomic distances R_{AB} as

$$E_{\mathrm{nn}} = \frac{1}{2}\sum_A \sum_{A\neq B} \frac{Z_A Z_B}{R_{AB}} \tag{12}$$

The repulsive character of E_{rep} is due to E_{nn}, which predominates over the double-counting terms. Similarly to E_0, E_{rep} does not depend on the electron density fluctuation $\Delta\rho$ and, therefore, is not a property of specific chemical environments.

On the basis of the work of Foulkes and Haydock,[25] E_{rep} can be conveniently approximated as a sum of diatomic contributions. They have defined the reference electron density as a superposition of atomic contributions centered at the nuclear positions, i.e.

$$\rho_0(\vec{r}) = \sum_A \rho_0^A(\vec{r} - \vec{R}_A) \tag{13}$$

such that the repulsion energy could be expanded as

$$E_{\mathrm{rep}}[\rho_0] = \sum_A E_{\mathrm{rep}}[\rho_0^A] + \frac{1}{2}\sum_A \sum_{B\neq A} \left(E_{\mathrm{rep}}[\rho_0^A + \rho_0^B] - E_{\mathrm{rep}}[\rho_0^A] - E_{\mathrm{rep}}[\rho_0^B]\right) + (\text{three- and higher-center interactions}) \tag{14}$$

The terms of more than two centers arise from exchange-correlation contributions and are expected to be negligible.[25] Thus, eq 14 can be truncated after the second term.

In principle, by truncating eq 14 after the second term, it is straightforward to calculate the repulsion energy from first principles. However, the result is typically frustratingly incorrect, in particular because of the large internuclear repulsion term, which is calculated exactly, whereas the compensating components that are functions of the electron density are subject to the DFTB approximations. Thus, E_{rep} is usually calculated from a force-field approximation designed to compensate for the various inaccuracies and approximations of DFTB. More specifically, eq 14 is typically written as a sum of diatomic potentials

$$E_{\mathrm{rep}} = \frac{1}{2}\sum_A \sum_{B\neq A} v_{\mathrm{rep}}^{AB}(R_{AB}) \tag{15}$$

with the v_{rep}^{AB} potentials conveniently represented as analytical functions of the interatomic distance R_{AB}, typically in the form of positive definite polynomials or splines that are fitted to the difference between DFT total energies and DFTB electronic energies E_{ele} (see eqs 1 and 9), calculated for one or more representative reference systems, finite or periodic. In this formulation, v_{rep}^{AB} normally diverges to large values as the interatomic distances become shorter than the equilibrium bond lengths. On the other hand, for interatomic distances increasing beyond the bond length values, v_{rep}^{AB} quickly converges to zero, usually vanishing before R_{AB} reaches the value of twice the bond length (i.e., the repulsion potential does not affect interactions with second neighbors). Although the values of v_{rep}^{AB} are appreciable, they are considerably smaller than the electronic energy E_{ele} in the range of bond lengths.

The advantage of parametrizing the repulsive energy as a two-body force field is obvious: as it is obtained for representative structures, often close to those of the application in mind, it compensates for all approximations and systematic errors made before. Also, the calculation of energies and energy gradients are computationally negligible compared to solving the secular problem defined by the DFTB equations. The disadvantage, however, is that it leads to relatively small coverage of systems with different chemical environments and to large manual efforts in the parametrization, since the parametrization of N elements requires $N(N + 1)/2$ pair potential fittings.

Here, we note that the only two-center quantity in eq 14 (restricted to the first two terms) is the interatomic distance R_{AB}, defined by the position of atoms A and B. Thus, instead of developing diatomic force fields by trying to match reference data, we explicitly calculate the E_{rep} contributions for each R_{AB} using the atomic electron densities ρ_0^A. As in the electronic term E_0, ρ_0^A is again a trial density, and we parametrize this quantity via the pseudoatomic calculation represented in eq 11. Two parameters, r_0^A and σ_A, defining the shape of the confinement potential in eq 10 are optimized to match a representative reference set (see Parametrization Details). As result, a

DOI: 10.1021/acs.jctc.5b00702
J. Chem. Theory Comput. 2015, 11, 5209−5218

complete DFTB parametrization requires only four parameters per element, in addition to the chosen exchange-correlation potential and the basis set.

3. PARAMETRIZATION DETAILS

In this work, we adopt the same strategy presented for the E_0 contribution in our previous article.[15] This means that atomic parameters defining E_{rep} are developed. Afterward, those are used to precalculate diatomic repulsion contributions E_{rep}^{AB} as a function of the interatomic distance R_{AB} for each pair of chemical elements A and B.

It should be noted that the E_{rep} contributions are optimized once the electronic parameters, i.e., the parameters necessary for E_0 and E_{scc}, have been chosen. In this work, we use the electronic parameters from the QUASINANO2013.1[15] set.

3.1. Calculation of the Atomic Electron Densities ρ_0^A. The atomic electron densities are calculated from spherically symmetric atomic orbitals ϕ_ν^A, calculated self-consistently according to eq 11, subject to the confinement potential defined in eq 10.

Following our previous work,[15] these calculations are performed using the PBE[26] exchange-correlation functional, with numerical atomic orbitals (NAOs) obtained with the Herman−Skillman procedure,[27] as implemented in the BAND2014[28−32] program.

Once the atomic orbitals ϕ_ν^A have been obtained, the atomic electron density is given by

$$\rho_0^A(\vec{r}) = \sum_\nu n_\nu |\phi_\nu^A(\vec{r})|^2 \tag{16}$$

where n_ν is the occupation number of the νth atomic energy level.

On the basis of the two-center approximation shown in eq 14, the E_{rep} part of eq 4 is rewritten as

$$E_{rep} \approx \frac{1}{2}\sum_A \sum_{B\neq A} E_{rep}^{AB} = \frac{1}{2}\sum_A \sum_{B\neq A} \left[-\frac{1}{2}\int\int \frac{(\rho_0^A(\vec{r}_A) + \rho_0^B(\vec{r}_B))(\rho_0^A(\vec{r}'_A) + \rho_0^B(\vec{r}'_B))}{|\vec{r} - \vec{r}'|} d\vec{r}\, d\vec{r}' + E_{xc}[\rho_0^A + \rho_0^B] - \int (\rho_0^A(\vec{r}_A) + \rho_0^B(\vec{r}_B)) v_{xc}\, d\vec{r} + \frac{Z_A Z_B}{R_{AB}} + C_{AB} \right]_{R_{AB}} \tag{17}$$

where the atomic densities are centered in their respective atoms, i.e., $\vec{r}_A = \vec{r} - \vec{R}_A$ and $\vec{r}'_A = \vec{r}' - \vec{R}_A$. In this equation, the exchange-correlation (XC) terms are calculated using the PBE[26] functional, as implemented in the BAND2014[28−32] program. Moreover, the XC terms are short-ranged and converge quickly with R_{AB}.

At long enough distances, the first term within the summation (Coulomb term) is exactly canceled by the internuclear repulsion term. However, because of the one-center terms embedded in the two-center integrals, E_{rep}^{AB} does not converge to zero. Thus, in practice, the value of the C_{AB} constants are determined empirically for each pair of elements by imposing the following limiting condition

$$\lim_{R_{AB}\to\infty} E_{rep}^{AB}(R_{AB}) = 0 \tag{18}$$

Consequently, the following rule applies

$$E_{rep}(R_{AB}) = 0,\ \forall\ R_{AB} \geq R_{AB}^{cut} \tag{19}$$

where R_{AB}^{cut} is the distance at which $E_{rep}^{AB}(R_{AB})$ reaches convergence.

3.2. Optimization of the Atomic Confinement Potentials. Except for Monte Carlo simulations, structural data is obtained by geometry optimization or by computation of molecular dynamics trajectories. Both methods heavily employ energy gradients. As obtaining high-quality structural data is the principal objective of this work, we optimize the parameters defining the confinement potential, and thus E_{rep}, based on reference geometries of allotropic systems.

For each element, the Nelder−Mead simplex method,[33] implemented in the SciPy 0.14.0 computing package,[34] is used to obtain the r_0 and σ values that minimize the atomic forces on the training geometries listed in Table 1. The procedure develops as follows:

(1) Calculation of $E_{rep}^{AB}(R_{AB})$ (here, A and B are indexes of different atoms of the same element) using an initial estimate of the confinement potential. In this case, we have used the electronic confinement potentials[15] as the starting point.
(2) For each training system, calculation of the maximum atomic force component using the candidate DFTB parameters.
(3) Calculation of the root-mean-square of the atomic forces obtained in the previous step. This is the quantity that has to be minimized.

Table 1. Training Systems Used in the Optimization of the Repulsion Energy Parameters[a]

Z	element	training systems
1	H	H_2, H_3^+
2	He	He_2, He (hcp)
3	Li	Li_2, Li (bcc), Li (fcc)
4	Be	Be_2, Be (hcp)
5	B	B (α-R), B_{40}, B_{80}
6	C	C_2, C (Carbyne), C (Diamond), C (Graphene), C (Pentagraphene)
7	N	N_2, N_4 (Tetraazacyclobutadiene), N_4 (Tetraazatetrahedrane), N_6 (Hexazine), N_8 (Octaazacubane), N_{10} (Bispentazole)
8	O	O_3 (Ozone), O_3 (Trioxirane), O_5 (Pentoxolane)
9	F	F_2
10	Ne	Ne_2, Ne (fcc)
11	Na	Na_2, Na (bcc), Na (hcp)
12	Mg	Mg_2, Mg (bcc), Mg (fcc), Mg (hcp)
13	Al	Al (fcc)
14	Si	Si_2 (singlet), Si (Diamond), Si (Silicene)
15	P	P_2, P_4 (Tetraphosphorus), P (Phosphorene)
16	S	S_2 (singlet), S_3, S_6 (Hexathiane), S_8 (Octathiocane)
17	Cl	Cl_2
18	Ar	Ar_2, Ar (fcc)
19	K	K_2, K (bcc), K (fcc)
20	Ca	Ca_2 Ca (bcc), Ca (fcc)
35	Br	Br_2

[a]The same confinement has been used for the electronic and repulsion contributions of He, Ne, and Ar.

DOI: 10.1021/acs.jctc.5b00702
J. Chem. Theory Comput. 2015, 11, 5209−5218

(4) If convergence has been achieved, then the final parameters are reported; otherwise, r_0 and σ are updated, and the procedure is repeated until convergence is reached.

Once the confinement parameters have been determined for each element, the repulsion energy between atoms of different elements is calculated without any further optimization.

In this work, we have restricted ourselves to the first 20 elements (H−Ca) of the periodic table. The reason is that, for many systems involving heavier atoms (i.e., the d-block), explicit treatment of spin polarization is needed. For even heavier atoms, the inclusion of spin−orbit coupling is required. Both spin polarization and spin−orbit coupling have been developed for DFTB by Köhler et al.[10,11] and implemented in the DFTB+ code.[35] Our parametrization tools, however, are based on a less diverse software implementation in which both DFTB extensions are not yet available. As both are scheduled for implementation, we are confident that repulsive potentials for the periodic table will be available soon. Nonetheless, the parametrization described in the present article comprises most commonly occurring elements and is sufficient to treat a large fraction of the systems in chemistry, physics, materials science, and biology.

3.3. Validation of the Optimized Parameters. The optimized DFTB parameters are validated using structural reference sets of allotropic and compound systems. A summary of each reference set used in this work is given in Table 2, whereas more detailed information can be found in the Supporting Information. In this work, we test the most popular DFTB variant, SCC-DFTB.[4] However, the same strategy can be applied to DFTB in its original, non-self-consistent form, as well as to the more recent DFTB variant, DFTB3.[12]

Table 2. Geometry Benchmark Sets[a]

name	size	description
Allotropes	68	Elementary substances, including periodic and nonperiodic species.
G2/97∪G3/05	225	MP2(full)/6-31G* geometries of closed-shell systems from the G2/97[36,37] and G3/05[38] test sets. In this work, the geometries have been used as obtained from the original publications.
G1G17	25	Alkali metal halides and diatomic molecules of hydrogen halides and alkali metal hydrides.
G2G16	12	Alkaline earth oxides and sulfides.
BN	5	Boron nitride compounds; except for diatomic BN, all systems are periodic.
SiO	6	Silicon oxides; diatomic SiO is the only nonperiodic system.

[a]Unless otherwise stated all geometries have been optimized with PBE/TZP.

Except for the structures in the *G2/97∪G3/05* set, which have been obtained elsewhere,[36−38] the reference geometries have been calculated using the PBE functional with the TZP basis sets, as implemented in ADF2014[39−41] (used for finite structures) and BAND2014[28−32] (used for the periodic structures). In the case of periodic structures, the lattice vectors have been optimized as well.

The performance of the SCC-DFTB calculations is evaluated by comparing the mean absolute percent deviations (MAPDs) and mean signed percent deviations (MSPD) of bond lengths and bond angles, with respect to the PBE/TZP geometries. For each reference structure, the MAPD is calculated as

$$\mathrm{MAPD} = \frac{1}{N}\sum_{i=1}^{N}\left|\frac{X_i^{\mathrm{dftb}} - X_i^{\mathrm{ref}}}{X_i^{\mathrm{ref}}}\right| \tag{20}$$

and the MSPD as

$$\mathrm{MSPD} = \frac{1}{N}\sum_{i=1}^{N}\frac{X_i^{\mathrm{dftb}} - X_i^{\mathrm{ref}}}{X_i^{\mathrm{ref}}} \tag{21}$$

where X_i are the values of the N bond lengths (or bond angles) of the test system.

It should be noted that, in principle, bond angles are determined by the electronic part of the DFTB Hamiltonian, which defines the type of the chemical bonds, and not by the repulsion potential. However, if the distance between two ligands (not bonded to each other) falls within the range of the corresponding repulsion potential, their interatomic distance will be affected by the repulsion and, consequently, the bond angles defined by those ligands might be affected as well. Therefore, poor description of bond angles could be an indication that both the repulsion potential and the electronic parameters should be reviewed.

The DFTB geometries have been calculated with the ADF DFTB 2014[42] program, using the geometries from the reference sets as initial coordinates. The default tolerance criteria defined in ADF DFTB 2014 have been used: 10^{-5} E_h for the total energy, 10^{-3} E_h Å^{-1} for the energy gradient, and 10^{-3} Å for the Cartesian coordinates. Geometries not converged within 150 optimization cycles have been counted as failed cases; in this situation, the MAPDs and MSPDs are not calculated.

A complete list of the test systems in the reference sets is provided in the Supporting Information, along with full data regarding the MAPD and MSPD calculations.

4. RESULTS AND DISCUSSION

The valence electron configurations as well as the E_{ele} and E_{rep} confinement potentials used in the QUASINANO2015 parameter set are shown in Table 3. The confinement potential parameters defining E_{ele} remain the same as those used in QUASINANO2013.1[15] set.

In order to evaluate the SCC-DFTB parameters, we focus on geometric properties. Below, we present benchmark geometry calculations with the QUASINANO2015 parameters, in comparison to MATSCI-0-3[18] and MIO-1-1[4,12,19] parameters. We also compare our results with the well-regarded PM7[20] semiempirical method. The SCC-DFTB calculations have been performed using the ADF DFTB 2014[42] program, whereas the PM7 calculations have been carried out with MOPAC[20,43] software. The full data obtained in this work is available as Supporting Information.

4.1. *Allotropes* Benchmarks. Most of the geometries in the *Allotropes* set (57 out of 68) have been explicitly used as references for the optimization of the QUASINANO2015 parameters. Hence, the *Allotropes* benchmarks do not allow conclusions regarding the transferability of the QUASINANO2015 parameters. However, since the errors are the smallest possible for QUASINANO2015, the *Allotropes* tests are appropriate for analyzing the level of accuracy that can be expected.

The MAPDs of bond lengths and bond angles are shown in Figure 1 for the *Allotropes* geometries. To facilitate the interpretation of the data, so-called Tukey boxplots[44] have been used.

DOI: 10.1021/acs.jctc.5b00702
J. Chem. Theory Comput. 2015, 11, 5209−5218

Table 3. Valence Electron Configurations and Confinement Potentials for the Electronic and Repulsion Energy Terms in the QUASINANO2015 Parameter Set

			E_{ele} conf.[a]		E_{rep} conf.	
Z	element	valence shell	r_0	σ	r_0	σ
1	H	$1s^1$	1.600	2.20	1.508	3.16
2	He	$1s^2$	1.400	11.40	1.400	11.40
3	Li	$2s^1\ 2p^0$	5.000	8.20	2.615	7.79
4	Be	$2s^2\ 2p^0$	3.400	13.20	1.990	8.31
5	B	$2s^2\ 2p^1$	3.000	10.40	2.087	11.98
6	C	$2s^2\ 2p^2$	3.200	8.20	2.142	7.86
7	N	$2s^2\ 2p^3$	3.400	13.40	2.196	12.83
8	O	$2s^2\ 2p^4$	3.100	12.40	1.921	14.70
9	F	$2s^2\ 2p^5$	2.700	10.60	1.907	11.88
10	Ne	$2s^2\ 2p^6$	3.200	15.40	3.200	15.40
11	Na	$3s^1\ 3p^0$	5.900	12.60	4.888	13.98
12	Mg	$3s^2\ 3p^0$	5.000	6.20	3.687	6.41
13	Al	$3s^2\ 3p^1\ 3d^0$	5.900	12.40	3.549	12.72
14	Si	$3s^2\ 3p^2\ 3d^0$	4.400	12.80	3.932	11.68
15	P	$3s^2\ 3p^3\ 3d^0$	4.000	9.60	3.080	9.84
16	S	$3s^2\ 3p^4\ 3d^0$	3.900	4.60	3.008	4.47
17	Cl	$3s^2\ 3p^5\ 3d^0$	3.800	9.00	3.163	8.69
18	Ar	$3s^2\ 3p^6\ 3d^0$	4.500	15.20	4.500	15.20
19	K	$4s^1\ 4p^0\ 3d^0$	6.500	15.80	6.097	16.20
20	Ca	$4s^2\ 4p^0\ 3d^0$	4.900	13.60	6.005	10.54
35	Br	$4s^2\ 4p^5\ 4d^0$	4.300	6.40	3.722	6.32

[a]The QUASINANO2013.1[15] confinement potentials have been used for the electronic contributions.

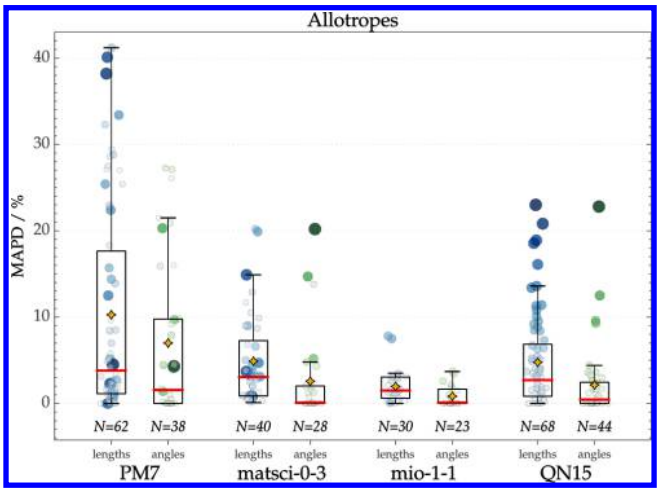

Figure 1. Boxplots of bond length and bond angle mean absolute percent deviations (MAPDs) within the *Allotropes* benchmark set. In each distribution, the size and color intensity of the data points are proportional to the corresponding MAPD values obtained with the QUASINANO2015 parameter set (QN15). The red bars represent the median values, whereas the yellow stars represent the mean values. The number of data points is shown below the respective boxplot.

In a Tukey boxplot, the data is represented by a vertical box in which the bottom and top lines are the first and third quartiles of the population, respectively. A horizontal line is placed inside the box, marking the median value (second quartile). Furthermore, whiskers are drawn to mark the lower and upper inner fences of the data distribution. These fences are, respectively, the lowest datum within 1.5 IQR of the lower quartile and the highest datum within 1.5 IQR of the highest quartile. In turn, the IQR is the interquartile range, i.e., the difference between the third and first quartiles (the height of the box). Finally, any datum not between the lower and upper inner fences is classified as an outlier. In an typical Tukey boxplot, only the outliers are explicitly shown; however, in this article, we have opted for plotting all of the data explicitly. In addition, we have also marked the mean values (Figure 1).

In comparison with MATSCI-0-3, the MAPD distributions obtained with QUASINANO2015 are practically identical. Regarding bond lengths, both parameter sets have their mean MAPD values at 5%. The median, third quartile, and upper inner fence MAPD values for QUASINANO2015 are, respectively, 3, 7, and 14%, which is very similar to the corresponding values in MATSCI-0-3. With respect to bond angles, both QUASINANO2015 and MATSCI-0-3 have mean MAPD at ca. 2 and 3%, respectively. The median, upper quartile, and upper inner fence of QUASINANO2015 are at 0, 3, and 4%, which differ by less than 1% from the corresponding values in MATSCI-0-3.

The main differences between the results obtained with QUASINANO2015 and MATSCI-0-3 are related to the number of parametrized interactions. The MATSCI-0-3 set contains parameters for only 40 of the 68 geometries in the *Allotropes* benchmark set. Thus, except for Al species, we verify that the outliers in the QUASINANO2015 MAPD distributions correspond to geometries that are not accessible to MATSCI-0-3, i.e., Li (fcc), Be_2, and Mg_2, or that are also outliers of MATSCI-0-3, i.e., Na (hcp), B_{40}, and B_{80}. Regarding Al species, all MAPDs are below 4% in MATSCI-0-3, whereas the smallest error with QUASINANO2015 is ca. 14% for Al (fcc) and ca. 20% for Al_2 molecules. On the other hand, it should be noted that, differently from QUASINANO2015, Na (bcc) appears as an outlier in MATSCI-0-3.

The best results are, however, those obtained with the MIO-1-1 parameters, as shown in Figure 1. The only outliers are H_3^+ and O_2^{2-}, both with bond length MAPD of ca. 8%. Moreover, the MAPD distribution of the bond lengths is rather symmetric, with the upper inner fence at ca. 4% and median and mean values at ca. 2%. However, it should be noted that, like MATSCI-0-3, the MIO-1-1 parameters are not defined for all tests in the *Allotropes* set. The MIO-1-1 parameters are restricted to only six elements, namely, H, C, N, O, P, and S. This translates into only 30 of the 68 species of the *Allotropes* benchmark set (less than half). In fact, if the QUASINANO2015 data is restricted to the cases where MIO-1-1 is applicable, then a very different MAPD distribution appears for the bond lengths: the mean and median values both become ca. 2%, with lower and upper quartiles at ca. 1 and 3%, respectively; the lower inner fence remains at zero, whereas the upper inner fence becomes ca. 4%, with H_3^+, N_2, and O_2^{2-} appearing as outliers. In other words, it gives a distribution very similar to that obtained with MIO-1-1.

A rather unexpected result is the MAPDs obtained with PM7. Although the median MAPD values for bond lengths and angles are below 5% (comparable to MATSCI-0-3 and QUASINANO2015), the upper half of the data is scattered along a wide range of values. In fact, the MAPD upper inner fence for bond lengths and angles are found, respectively, at ca. 41 and 21% with PM7. These larger MAPD values seem to be particularly related to alkali metal species, aluminum, and periodic systems of carbon and phosphorus.

4.2. *G2/97∪G3/05* Benchmarks. Figure 2 shows the MAPDs of bond lengths and bond angles, with respect to MP2(full)/6-31G* geometries of the closed-shell systems from the G2/97[36,37] and G3/05[38] test sets. A total of 225 geometries

DOI: 10.1021/acs.jctc.5b00702
J. Chem. Theory Comput. 2015, 11, 5209−5218

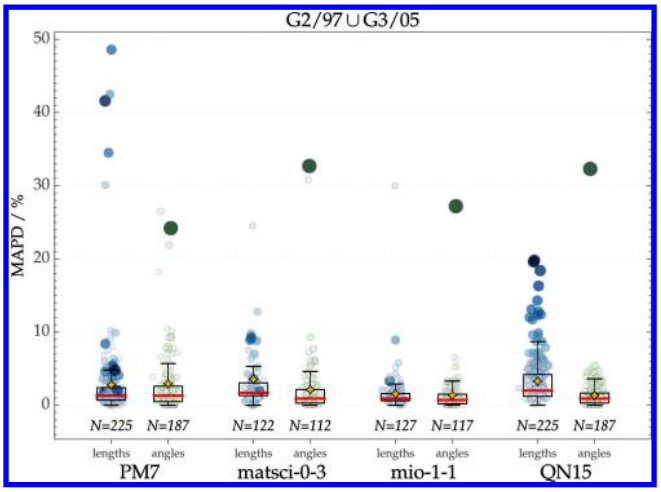

Figure 2. Boxplots of bond length and bond angle mean absolute percent deviations (MAPDs) within the *Allotropes* benchmark set. In each distribution, the size and color intensity of the data points are proportional to the corresponding MAPD values obtained with the QUASINANO2015 parameter set (QN15). The red bars represent the median values, whereas the yellow stars represent the mean values. The number of data points is shown below the respective boxplot. Data not shown: 94% bond angle MAPD for SiH_2 (silylene) with PM7 and 121% bond length MAPD for O_3 with MATSCI-0-3.

has been included, comprising all of the chemical elements parametrized in this work, except for the noble gases (He, Ne, and Ar) and Ca. It should be noted that for a few elements, namely, the alkali metals (Li, Na, and K), Be, Mg, B, and Al, very few geometries (five or less) are available within the G2/97 and G3/05 sets. Nevertheless, these sets still provide a very good reference for the transferability and accuracy of the QUASINANO2015 parameters.

Within the *G2/97∪G3/05* test set, the Tukey boxplots become more comparable among all calculations. Regarding bond angles, all calculations have mean MAPD values lower than 3%, with upper inner fences below 6%. In general, even the outliers are below or near 10%. One systematic exception is the NH_2^+ cation, which appears with bond angle MAPDs above 20% in all calculations.

The MAPD distribution of the bond lengths calculated with PM7, MATSCI-0-3, and MIO-1-1 are better than the distribution obtained with QUASINANO2015. However, except for the outliers, this discrepancy is not too large. The MAPD mean values are between 2 and 4% for all calculations, and the MAPD median values are between 1 and 2%. The third quartile of QUASINANO2015 is comparable to the upper inner fence of MATSCI-0-3; however, the upper inner fence of QUASINANO2015 is still below 10%.

As observed in the *Allotropes* test set, the outliers of QUASINANO2015 either are outliers in the MATSCI-0-3 and MIO-1-1 distributions (H_3^+, SiO, Si_2H_2, SiH_5^+) or are not defined within these parameter sets (e.g., compounds of alkali metals or halogens). On the other hand, many outliers of MATSCI-0-3 and MIO-1-1 are better or equivalently described by QUASINANO2015 (e.g., HNO, N_2O_4, $H_2C{=}CH^+$). In particular, a MAPD of ca. 121% has been obtained with MATSCI-0-3, whereas the same value is less than 2% with QUASINANO2015.

Differently from the *Allotropes* test set, the geometries in *G2/97∪G3/05* are very well-described with PM7. However, it is difficult to absolutely state that PM7 performs better than QUASINANO2015. Although the distribution of bond length MAPDs is more disperse for QUASINANO2015, the outliers have considerably larger errors in PM7. In addition, the distribution of the errors for bond angles is better in QUASINANO2015.

Overall, the performance of the QUASINANO2015 parameters regarding geometries is comparable to that of PM7, MATSCI-0-3, and MIO-1-1. The outliers indicate that the shortcomings of QUASINANO2015 are especially related to Al and fluorides, although some species (e.g., H_3^+) also show relatively high MAPDs.

4.3. *G1G17* and *G2G16* Benchmarks. The *G2/97∪G3/05* test set covers a large amount of element combinations and local chemical environments. However, these sets are clearly skewed toward organic molecules and do not include any periodic system. The *G1G17* and *G2G16*, on the other hand, consist of inorganic compounds only, with geometries optimized using the PBE[26] exchange-correlation functional and TZP basis set, as implemented in BAND2014.[28−32]

The *G1G17* test set comprises bulk crystals and diatomic molecules of alkali metal halides, as well as diatomic molecules of alkali metal hydrides and hydrogen halides. For the bond lengths, the MAPDs obtained with QUASINANO2015 are evenly distributed from zero to ca. 18%, with the median value at ca. 7%. For Na and K, the fluorides have MAPDs higher than 10%, whereas the chlorides and bromides have MAPDs lower than 7%. This pattern is inverted for Li; in this case, the fluorides are better described, with MAPDs lower than 4%, whereas the chlorides and bromides have MAPDs higher than 10%. Regarding the molecules with hydrogen, only HCl and HBr are well-described with QUASINANO2015. In comparison, all systems are generally well-described with PM7, except for LiF (fcc) (geometry did not converge), Na_2Cl_2 (ca. 12% bond angle MAPD), NaH (ca. 20% MAPD), and LiH (ca. 41% MAPD). Neither the MATSCI-0-3 nor the MIO-1-1 set has the necessary parameters for the *G1G17* test set.

The *G2G16* test set has been constructed with the same principles as those of *G1G17*. It contains bulk systems and diatomic molecules of oxides and sulfides of Be, Mg, and Ca. The MAPDs of bond angles are generally close to zero with both QUASINANO2015 and PM7, except for CaO (fcc) and MgO (fcc). The former has bond angle MAPD of ca. 16% with PM7, whereas the latter has bond angle MAPD of 10%. Regarding the bond lengths, although the Be compounds are better described with PM7, the MAPDs obtained with QUASINANO2015 are all bellow 8%. For the Mg compounds, on the other hand, QUASINANO2015 performs better, with MAPDs below 3%, with the exception of MgO (fcc) mentioned above. The highest MAPDs are found for the Ca compounds, starting at ca. 8% for CaS (fcc), up to ca. 25% for CaO. However, PM7 also exhibits a large dispersion of the data for Ca, from zero up to 16% bond length MAPDs. As for the *G1G17* set, neither the MATSCI-0-3 nor the MIO-1-1 set has the necessary parameters for the *G2G16* test set.

4.4. *BN* and *SiO* Benchmarks. The results obtained with MATSCI-0-3 and QUASINANO2015 for the boron nitrides are very similar. The MAPDs are lower than 4% for bond lengths and lower than 1% for the bond angles. The only exception is trigonal $B_{13}N_2$. In this case, the bond length MAPD is 6% with MATSCI-0-3 and ca. 11% with QUASINANO2015, whereas the MAPDs of the bond angles are 6 and 7%, respectively. Nevertheless, given the complexity of the $B_{13}N_2$ geometry, this can still be considered a good result.

DOI: 10.1021/acs.jctc.5b00702
J. Chem. Theory Comput. 2015, 11, 5209−5218

Table 4. Isomerization Energies (kcal mol^{-1}) of Selected Hydrocarbons[a]

Reaction	Exp.[45]	PBE/TZP	PM7	MATSCI-0-3	MIO-1-1	QN15
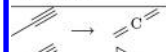	1.24	-2.76	-9.13	9.60	6.18	9.93
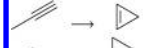	21.81	19.98	17.22	53.44	38.67	60.11
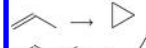	7.85	6.26	7.83	23.81	13.34	23.73
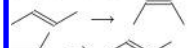	1.13	1.11	1.19	-0.50	0.96	-0.11
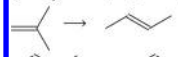	1.27	0.41	0.56	-1.14	1.00	-1.70
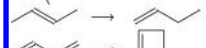	2.79	3.45	4.69	3.00	4.10	4.16
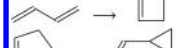	11.34	10.65	10.02	10.09	12.87	14.92
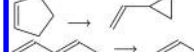	22.17	21.12	23.11	54.10	34.94	51.90
	7.13	8.83	5.21	8.01	8.51	9.83
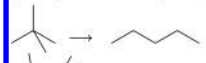	5.06	1.32	2.24	-4.95	1.81	-6.26
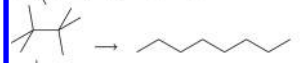	4.09	-5.31	-1.18	-9.57	-1.05	-13.41
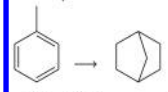	46.65	50.50	45.94	50.52	49.68	68.18
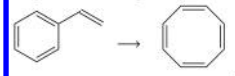	35.83	39.16	22.51	40.43	44.45	44.41
MAE	—	2.52	3.38	9.72	4.98	12.57

[a]Zero-point energy and thermal corrections not included.

Regarding silicon oxides, the QUASINANO2015 parameters systematically overestimate the Si−O bond lengths. In each test, the MAPD and MSPD of the bond lengths have exactly the same value (between 11 and 14%), with the MAPDs of bond angles being always lower than 3%. Hence, although Si−O is overestimated, the crystals are not distorted and a qualitative description is still achieved. Nevertheless, it should be noted that the bond length MAPDs obtained with MATSCI-0-3 are lower than 3%, indicating it should be possible to improve the QUASINANO2015 parameters for silicon oxides.

4.5. Isomerization Energies of Selected Hydrocarbons. In order to estimate how well (or how poorly) the QUASINANO2015 parameters would perform outside of their parametrization scope, we have calculated the isomerization energies of selected hydrocarbons (Table 4). We have not included zero-point energy or thermal corrections, as they are not expected to significantly affect the mean average deviation (MAD) values.[45]

As shown in Table 4, a MAD of ca. 13 kcal mol^{-1} has been obtained for the isomerization energies calculated with the QUASINANO2015 parameters, in comparison with only ca. 5 kcal mol^{-1} for the MIO-1-1 set and ca. 3 kcal mol^{-1} for both PM7 and PBE/TZP. The relatively high MAD obtained for QUASINANO2015 is expected, as energetic properties have not been explicitly included in the parametrization procedure. However, it is interesting to notice that the performance of QUASINANO2015 is comparable to the performance of the MATSCI-0-3 set, for which a MAD of ca. 10 kcal mol^{-1} has been obtained. These results show that, as expected, the parameters presented in this work are not accurate enough for the calculation of energetic properties. However, the inaccuracy is not inherent of the DFTB method, as evidenced by the MIO-1-1 results; thus, the algorithm presented here can be easily adapted for obtaining accurate parameters for energetic properties.

5. CONCLUSIONS

We have developed an automatic parametrization method for the DFTB repulsion energy contributions. In this method, the repulsion energy is calculated directly from the KS-like energy distributions, with trial densities obtained from DFTB pseudoatoms subject to a confinement potential. The shape of the confinement potential is defined by two free parameters, governing its width and curvature.

Using the methodology described in this work, we have constructed the QUASINANO2015 parameter table, comprising the first 20 elements of the periodic table (H to Ca) as well as Br, on top of the electronic parameters from QUASINANO2013.1.[15] It is very important to note that the only independent parameters that are needed to define our DFTB approach are, besides the atomic configuration of the reference atom, four real numbers per element: two numbers to define the confinement potential for the electronic structure and two numbers to define the confinement potential for the repulsive energy terms. Everything else follows directly from the DFTB KS-like equations and can be calculated directly from DFTB using suitable software.

The QUASINANO2015 set has been tested for geometry optimization calculations. A large number of reference geometries (calculated with either PBE/TZP or MP2(full)/6-31G*) has been used to assess the performance of our DFTB parameters. Although a few elements and interactions could not be generally well described (e.g., Al, Ca, and Si−O bonds), reasonable accuracy and transferability have been achieved. Where direct comparison was possible, we have found that the performance of the QUASINANO2015 can be comparable to the performance of extensively tested parameters, namely, MATSCI-0-3[18] and MIO-1-1,[4,12,19] with few exceptions.

The results obtained for some elements indicate that improvements are still necessary. For instance, elementary species of Be, B, and Al have yielded considerably high MAPD values. However, when combined with other elements, better results have been achieved (e.g., for boron nitrides). On the other hand, small errors have been obtained for allotropes of Si and Ca, whereas calcium halides and silicon oxides have shown large deviations. It is possible that these problems could be minimized with the reoptimization of the repulsion parameters

DOI: 10.1021/acs.jctc.5b00702
J. Chem. Theory Comput. 2015, 11, 5209−5218

(using different reference structures) or even with the reoptimization of the electronic parameters. However, as an approximated method, DFTB is expected to pose intrinsic limits to the accuracy and transferability of its parameters.

It should be noted that the methodology presented in this work can be easily modified for obtaining DFTB parameters specifically optimized for other properties, such as reaction energies and vibrational frequencies. Moreover, as a general-purpose parameter set, additional corrections could be easily included in order to adapt these parameters to specific situations (e.g., additional force-field-like corrections, obtained on-the-fly for specific training systems). Nevertheless, it should be stressed that the parameters presented here have been optimized for structural properties only and are not expected to yield accurate results regarding other properties.

■ ASSOCIATED CONTENT

Supporting Information

The Supporting Information is available free of charge on the ACS Publications website at DOI: 10.1021/acs.jctc.5b00702.

Detailed description of the benchmark sets and plots of MAPD and MSPD distributions for bond lengths and bond angles (PDF)

All MAPD and MSPD values calculated in this work (XLSX)

■ AUTHOR INFORMATION

Corresponding Author

*E-mail: thomas.heine@uni-leipzig.de.

Funding

We acknowledge the financial support of the European Commission via the Marie Curie IAPP QUASINANO (GA 251149), the Marie Curie ITN-EID PROPAGATE (GA 316897), and the ERC Starting Grant C3ENV (GA 256962) projects.

Notes

The authors declare no competing financial interest.

■ ACKNOWLEDGMENTS

We thank Maximilian Schallwig for technical support regarding the preparation of reference geometry files. We also thank Agnieszka Kuc, André Mirtschink, Bálint Aradi, Gotthard Seifert, Fedor Goumans, Hans van Schoot, Mirko Franchini, Olivier Visser, and Stan van Gisbergen for enlightening discussions and support.

■ REFERENCES

(1) Seifert, G.; Eschrig, H.; Bieger, W. Z. *Z. Phys. Chem.* **1986**, *267*, 529−539.

(2) Hohenberg, P.; Kohn, W. *Phys. Rev.* **1964**, *136*, B864−B871.

(3) Kohn, W.; Sham, L. J. *Phys. Rev.* **1965**, *140*, A1133−A1138.

(4) Elstner, M.; Porezag, D.; Jungnickel, G.; Elsner, J.; Haugk, M.; Frauenheim, T.; Suhai, S.; Seifert, G. *Phys. Rev. B: Condens. Matter Mater. Phys.* **1998**, *58*, 7260−7268.

(5) Elstner, M.; Hobza, P.; Frauenheim, T.; Suhai, S.; Kaxiras, E. *J. Chem. Phys.* **2001**, *114*, 5149−5155.

(6) Zhechkov, L.; Heine, T.; Patchkovskii, S.; Seifert, G.; Duarte, H. A. *J. Chem. Theory Comput.* **2005**, *1*, 841−847.

(7) Grimme, S. *J. Comput. Chem.* **2006**, *27*, 1787−1799.

(8) Grimme, S.; Ehrlich, S.; Goerigk, L. *J. Comput. Chem.* **2011**, *32*, 1456−1465.

(9) Kim, H.; Choi, J.-M.; Goddard, W. A., III *J. Phys. Chem. Lett.* **2012**, *3*, 360−363.

(10) Köhler, C.; Seifert, G.; Frauenheim, T. *Chem. Phys.* **2005**, *309*, 23−31.

(11) Köhler, C.; Frauenheim, T.; Hourahine, B.; Seifert, G.; Sternberg, M. *J. Phys. Chem. A* **2007**, *111*, 5622−5629.

(12) Gaus, M.; Cui, Q.; Elstner, M. *J. Chem. Theory Comput.* **2011**, *7*, 931−948.

(13) Gaus, M.; Goez, A.; Elstner, M. *J. Chem. Theory Comput.* **2013**, *9*, 338−354.

(14) Kubillus, M.; Kubař, T.; Gaus, M.; Řezáč, J.; Elstner, M. *J. Chem. Theory Comput.* **2015**, *11*, 332−342.

(15) Wahiduzzaman, M.; Oliveira, A. F.; Philipsen, P.; Zhechkov, L.; van Lenthe, E.; Witek, H. A.; Heine, T. *J. Chem. Theory Comput.* **2013**, *9*, 4006−4017.

(16) Mirtschink, A. Berechnungen von Bindungsenergien zweiatomiger Moleküle der Elemente der ersten und zweiten Periode im Rahmen der DFTB-Methode. M.Sc. Thesis, Technische Universität Dresden, Germany, 2009.

(17) Bodrog, Z. Improvements to the Density-Functional Tight-Binding method: new, efficient parametrization schemes and prospects of a more precise self-consistency. Ph.D. Thesis, Universität Bremen, Germany, 2012.

(18) Frenzel, J.; Oliveira, A. F.; Jardillier, N.; Heine, T.; Seifert, G. Semi-relativistic, self-consistent charge Slater-Koster tables for density-functional based tight-binding (DFTB) for materials science simulations, 2009. http://www.dftb.org/parameters/download/matsci/matsci-0-3.

(19) Niehaus, T. *J. Mol. Struct.: THEOCHEM* **2001**, *541*, 185−194.

(20) Stewart, J. J. P. *J. Mol. Model.* **2013**, *19*, 1−32.

(21) Koskinen, P.; Mäkinen, V. *Comput. Mater. Sci.* **2009**, *47*, 237−253.

(22) Oliveira, A. F.; Seifert, G.; Heine, T.; Duarte, H. A. *J. Braz. Chem. Soc.* **2009**, *20*, 1193−1205.

(23) Elstner, M.; Seifert, G. *Philos. Trans. R. Soc., A* **2014**, *372*, 20120483.

(24) Janak, J. F. *Phys. Rev. B: Condens. Matter Mater. Phys.* **1978**, *18*, 7165−7168.

(25) Foulkes, W. M. C.; Haydock, R. *Phys. Rev. B: Condens. Matter Mater. Phys.* **1989**, *39*, 12520−12536.

(26) Perdew, J.; Burke, K.; Ernzerhof, M. *Phys. Rev. Lett.* **1996**, *77*, 3865−3868.

(27) Herman, F.; Skillman, S. *Atomic Structure Calculations*; Prentice-Hall: Englewood Cliffs, NJ, 1963.

(28) Philipsen, P. H. T.; te Velde, G.; Baerends, E. J.; Berger, J. A.; de Boeij, P. L.; Franchini, M.; Groeneveld, J. A.; Kadantsev, E. S.; Klooster, R.; Kootstra, F.; Romaniello, P.; Skachkov, D. G.; Snijders, J. G.; Verzijl, C. J. O.; Wiesenekker, G.; Ziegler, T. *BAND2014*; SCM, Theoretical Chemistry, Vrije Universiteit: Amsterdam, The Netherlands, 2014.

(29) te Velde, G.; Baerends, E. J. *Phys. Rev. B: Condens. Matter Mater. Phys.* **1991**, *44*, 7888−7903.

(30) Wiesenekker, G.; Baerends, E. J. *J. Phys.: Condens. Matter* **1991**, *3*, 6721−6742.

(31) Franchini, M.; Philipsen, P. H. T.; Visscher, L. *J. Comput. Chem.* **2013**, *34*, 1819−1827.

(32) Franchini, M.; Philipsen, P. H. T.; van Lenthe, E.; Visscher, L. *J. Chem. Theory Comput.* **2014**, *10*, 1994−2004.

(33) Nelder, J. A.; Mead, R. *Comput. J.* **1965**, *7*, 308−313.

(34) Jones, E.; Oliphant, T.; Peterson, P.; et al., *SciPy*: Open source scientific tools for Python, 2001. http://www.scipy.org/.

(35) Aradi, B.; Hourahine, B.; Frauenheim, T. *J. Phys. Chem. A* **2007**, *111*, 5678−5684.

(36) Curtiss, L. A.; Raghavachari, K.; Redfern, P. C.; Pople, J. A. *J. Chem. Phys.* **1997**, *106*, 1063−1079.

(37) Curtiss, L. A.; Redfern, P. C.; Raghavachari, K.; Pople, J. A. *J. Chem. Phys.* **1998**, *109*, 42−55.

(38) Curtiss, L. A.; Redfern, P. C.; Raghavachari, K. *J. Chem. Phys.* **2005**, *123*, 124107.

(39) Baerends, E. J.; Ziegler, T.; Autschbach, J.; Bashford, D.; Bérces, A.; Bickelhaupt, F. M.; Bo, C.; Boerrigter, P. M.; Cavallo, L.; Chong,

D. P.; Deng, L.; Dickson, R. M.; Ellis, D. E.; van Faassen, M.; Fan, L.; Fischer, T. H.; Fonseca Guerra, C.; Franchini, M.; Ghysels, A.; Giammona, A.; van Gisbergen, S. J. A.; Götz, A. W.; Groeneveld, J. A.; Gritsenko, O. V.; Grüning, M.; Gusarov, S.; Harris, F. E.; van den Hoek, P.; Jacob, C. R.; Jacobsen, H.; Jensen, L.; Kaminski, J. W.; van Kessel, G.; Kootstra, F.; Kovalenko, A.; Krykunov, M. V.; van Lenthe, E.; McCormack, D. A.; Michalak, A.; Mitoraj, M.; Morton, S. M.; Neugebauer, J.; Nicu, V. P.; Noodleman, L.; Osinga, V. P.; Patchkovskii, S.; Pavanello, M.; Philipsen, P. H. T.; Post, D.; Pye, C. C.; Ravenek, W.; Rodr'iguez, J. I.; Ros, P.; Schipper, P. R. T.; van Schoot, H.; Schreckenbach, G.; Seldenthuis, J. S.; Seth, M.; Snijders, J. G.; Solà, M.; Swart, M.; Swerhone, D.; te Velde, G.; Vernooijs, P.; Versluis, L.; Visscher, L.; Visser, O.; Wang, F.; Wesolowski, T. A.; van Wezenbeek, E. M.; Wiesenekker, G.; Wolff, S. K.; Woo, T. K.; Yakovlev, A. L. *ADF2014*; SCM, Theoretical Chemistry, Vrije Universiteit: Amsterdam, The Netherlands, 2014.

(40) Guerra, C. F.; Snijders, J. G.; te Velde, G.; Baerends, E. J. *Theor. Chem. Acc.* **1998**, *99*, 391−403.

(41) te Velde, G.; Bickelhaupt, F. M.; Baerends, E. J.; Guerra, C. F.; Van Gisbergen, S.; Snijders, J. G.; Ziegler, T. *J. Comput. Chem.* **2001**, *22*, 931−967.

(42) Yakovlev, A.; Philipsen, P.; Borini, S.; Rüger, R.; de Reus, M.; Ghorbani-Asl, M.; McCormack, D.; Patchkovskii, S.; Heine, T. *ADF DFTB 2014*; SCM, Theoretical Chemistry, Vrije Universiteit: Amsterdam, The Netherlands, 2014.

(43) Stewart, J. J. P. *MOPAC2012*; Stewart Computational Chemistry: Colorado Springs, CO, 2012.

(44) Tukey, J. W. *Exploratory Data Analysis*; Addison Wesley Pub. Co.: Reading, MA, 1977.

(45) Sattelmeyer, K. W.; Tirado-Rives, J.; Jorgensen, W. L. *J. Phys. Chem. A* **2006**, *110*, 13551−13559.

DOI: 10.1021/acs.jctc.5b00702
J. Chem. Theory Comput. 2015, 11, 5209−5218